The structure of the O2–N2O complex

Steven R. Salmon and Joseph R. Lane

Citation: The Journal of Chemical Physics **143**, 124303 (2015); doi: 10.1063/1.4931629
View online: http://dx.doi.org/10.1063/1.4931629
View Table of Contents: http://scitation.aip.org/content/aip/journal/jcp/143/12?ver=pdfcov
Published by the AIP Publishing

The structure of the O_2–N_2O complex

Steven R. Salmon and Joseph R. Lane[a)]
School of Science, Faculty of Science and Engineering, University of Waikato, Private Bag 3105, Hamilton 3240, New Zealand

(Received 14 May 2015; accepted 11 September 2015; published online 25 September 2015)

We have investigated the lowest energy structures and interaction energies of the oxygen nitrous oxide complex (O_2–N_2O) using explicitly correlated coupled cluster theory. We find that the intermolecular potential energy surface of O_2–N_2O is very flat, with two minima of comparable energy separated by a low energy first order saddle point. Our results are able to conclusively distinguish between the two sets of experimental geometric parameters for O_2–N_2O that were previously determined from rotationally resolved infrared spectra. The global minimum structure of O_2–N_2O is therefore found to be planar with a distorted slipped parallel structure. Finally, we show that the very flat potential energy surface of O_2–N_2O is problematic when evaluating vibrational frequencies with a numerical Hessian and that consideration should be given as to whether results might change if the step-size is varied. © *2015 AIP Publishing LLC.* [http://dx.doi.org/10.1063/1.4931629]

INTRODUCTION

Nitrous oxide (N_2O) is an atmospheric trace gas of paramount importance. It is now the dominant stratospheric ozone-depleting substance[1] and the third most significant greenhouse gas after carbon dioxide and methane.[2] However, despite its long-recognized importance, the global atmospheric budget of N_2O remains poorly quantified in terms of emission sources and sinks.[3,4] The concentration of N_2O is steadily increasing in the atmosphere and is presently 19% higher than pre-industrial levels.[5] Globally, natural sources of atmospheric N_2O account for 50%-70% of total emissions and arise primarily from bacterial processes in soils and the ocean.[2] Human activities are responsible for the remaining 50%-30% of N_2O emissions, with agricultural practices such as fertilizer use, land cultivation, and distribution of livestock manure to pasture, the primary cause.[2]

Nitrous oxide has a long atmospheric lifetime that is estimated to be 100-150 yr.[6] Photodissociation is the primary loss process for N_2O in the atmosphere [$N_2O \rightarrow N_2 + O(^1D)$], which occurs due to absorption of solar radiation in the stratospheric ultra-violet (UV) window from 185-230 nm:[7] This spectral region corresponds to the red shoulder of an extremely weak ($X\ ^1A' \rightarrow 2^1A'$) electronic transition in N_2O that is centred at 180 nm and has a broad Gaussian band shape.[7] This absorption band is symmetry-forbidden but couples to the non-symmetric vibrational bending mode of N_2O.[8] Changes to the vibrational modes of N_2O due to isotopic substitution are known to affect the photodissociation rate of N_2O.[9]

It is well established that weakly bound complexes are important for describing the chemistry of Earth's atmosphere.[10] As an example, the formation of oxygen dimer (O_2–O_2) facilitates photodissociation of O_2 with lower energy photons than for individual O_2 molecules.[11] We propose that formation of the N_2O–O_2 complex may also affect the photodissociation dynamics of N_2O in Earth's atmosphere by altering the vibrational modes of N_2O that couple to the symmetry-forbidden electronic transition. However, there have been only limited previous studies of this complex and as we will show, the presently accepted lowest energy structure is likely to be incorrect.

The O_2–N_2O complex was first studied experimentally by low-resolution infrared spectroscopy using matrix isolation techniques.[12] Additional weak absorption bands were observed in the ν_1 and ν_3 regions of N_2O, which were assigned to the O_2–N_2O complex. Qian *et al.* subsequently used supersonic expansion techniques to record the high-resolution infrared spectra of O_2–N_2O in the ν_3 region of N_2O.[13] These rotationally resolved spectra were used to determine the structure of O_2–N_2O, although two sets of geometric parameters were found to fit the data equally well. Consequently, they also calculated an empirical intermolecular potential energy surface to help assign the structure. Very recently, Li *et al.* recorded high-resolution infrared spectra of O_2–N_2O in the ν_1 region of N_2O.[14] While rotational constants were measured, only a limited structural analysis was completed that yielded an intermolecular distance that is consistent with the earlier work of Qian *et al.*

In this work, we investigate the lowest energy structures of the O_2–N_2O complex with the explicitly correlated unrestricted coupled cluster singles doubles and perturbative triples [UCCSD(T)-F12b] method. We construct an *ab initio* intermolecular potential energy surface using fixed monomer geometries to identify possible minima structures. We then optimize each of these minima allowing full geometric relaxation. Finally, we calculate vibrational harmonic frequencies to ensure that our optimized structures are indeed minima. We compare our results to the available experimental structural data obtained from rotationally resolved infrared spectroscopy.[13]

THEORETICAL METHODS

We have fully optimised the geometry of the O_2–N_2O complex and its constituent monomers with the explicitly

a)Electronic address: jlane@waikato.ac.nz

correlated UCCSD(T)-F12b method as implemented in MOLPRO2012.1.[15] All calculations were completed in the respective ground electronic states, i.e., $^3\Sigma_g^-$ for O_2 and $^1\Sigma^+$ for N_2O. A restricted open-shell Hartree-Fock (ROHF) reference was used for O_2–N_2O and O_2 whereas the restricted Hartree-Fock (RHF) reference was used for N_2O.

The geometry of the complex was optimised with both a standard optimization scheme and a counterpoise (CP) corrected optimization scheme to reduce the effects of basis set superposition error (BSSE).[16] We have used both the cc-pVTZ-F12 and the aug-cc-pVTZ orbital basis sets. The former have been specifically optimized for use with explicitly correlated F12 methods and are of similar size to the latter but contain fewer diffuse basis functions.

There are several variants of CCSD(T)-F12 available in MOLPRO 2012.1 that use different approximations for the CCSD-F12 component and the same triples component.[15] We have chosen to use the CCSD(T)-F12b method as the CCSD-F12b approximation demonstrates systematic convergence of the correlation energy with increasing basis set size.[17] The values of the geminal Slater exponent β were 0.9, 1.0, and 1.1 for the cc-pVDZ-F12, cc-pVTZ-F12, and cc-pVQZ-F12 basis sets and 1.0, 1.2, and 1.4 for aug-cc-pVDZ, aug-cc-pVTZ, and aug-cc-pVQZ basis sets, respectively.

We have extrapolated the CCSD(T)-F12b correlation energies to the complete basis set (CBS) limit using the approach of Schwenke,[18]

$$E_{CBS}^{corr} = (E_Y^{corr} - E_X^{corr})F_{XY}^{corr} + E_X^{corr}, \quad (1)$$

where E_X^{corr} and E_Y^{corr} are the correlation energies obtained with the smaller (X) and larger (Y) basis sets and F_{XY}^{corr} is the correlation factor. We extrapolate the CCSD-F12b and (T) contributions separately using the correlation factors determined by Hill *et al.* and add this to the HF complementary auxiliary basis set (CABS) energy obtained with the Y basis set.[17] The energies of the complexes are counterpoise corrected before extrapolation to the CBS limit.

All coupled cluster calculations assume a frozen core (N:1s; O:1s;). The optimization threshold criteria were set to gradient = 1×10^{-8} a.u., stepsize = 1×10^{-8} a.u., and energy = 1×10^{-10} a.u., with all single point energies converged to energy = 1×10^{-10} a.u., orbital = 1×10^{-9} a.u., coeff = 1×10^{-9} a.u., and the Hartree-Fock density matrix converged to accu = 1×10^{-20} a.u.

To confirm that our optimised stationary points are in fact minima, we have calculated harmonic vibrational frequencies with the CCSD(T)-F12b method.

RESULTS AND DISCUSSION

Potential energy surface

Previous high-resolution infrared spectra of the O_2–N_2O complex are consistent with a planar structure.[13,14] If we assume only minor geometric changes upon complexation, then the structure of O_2–N_2O can be described in terms of the Jacobi coordinates R_{cm}, θ_1, and θ_2, as shown in Figure 1.

In Figure 2, we present the CP corrected CCSD(T)-F12b/aug-cc-pVTZ potential energy surface (PES) of O_2–N_2O as a function of the Jacobi coordinates with a fixed intermolecular distance of 3.423 Å. The PES was constructed from single point energies from θ_1 = 35°-155° in 10° steps and θ_2 = 40°-130° in 7.5° steps. The PES is expressed relative to the energy of the two monomers at infinite separation hence negative values represent attractive regions of the PES and positive values represent repulsive regions of the PES. Two minima are evident on the potential energy surface, with either θ_1 = 122° and θ_2 = 104° or θ_1 = 52° and θ_2 = 83°. The former is the lower energy global minimum (−264 cm^{-1}) whereas the latter is a local minimum (−239 cm^{-1}). The two minima are separated by a first order saddle point at θ_1 = 103° and θ_2 = 79° with an energy of −196 cm^{-1}. The potential energy surface surrounding the two minima and the first order saddle

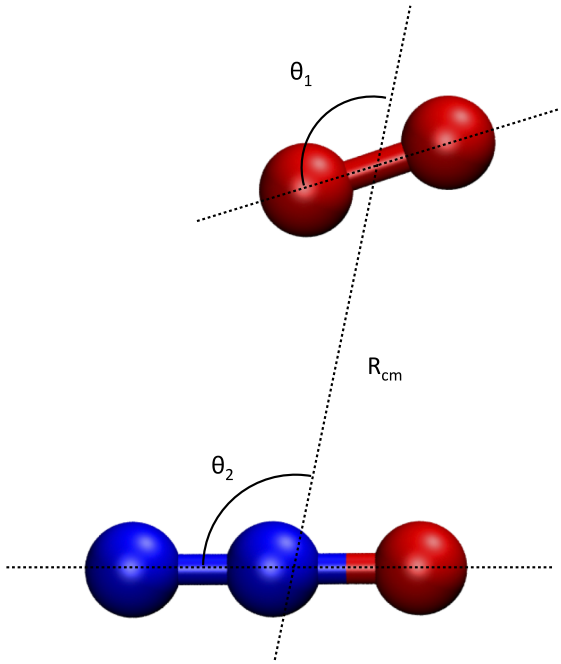

FIG. 1. Jacobi coordinates for O_2–N_2O using the nomenclature from Ref. 13.

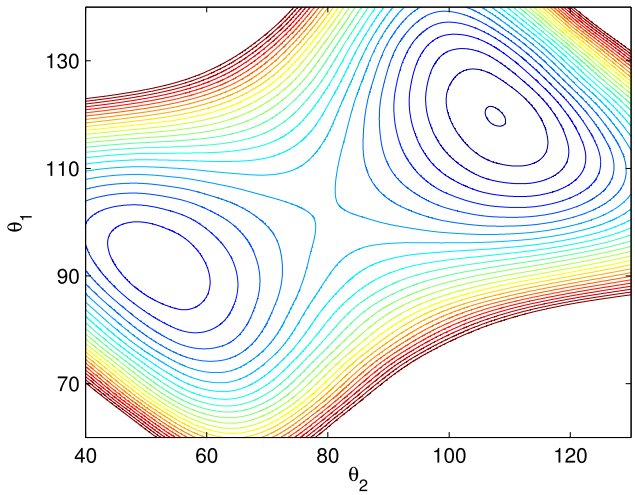

FIG. 2. The CP corrected CCSD(T)-F12b/aug-cc-pVTZ potential energy surface of O_2–N_2O. Results are obtained as a function of θ_1 and θ_2 with a fixed value of R_{cm} = 3.423 Å. Energies are expressed relative to the two monomers at infinite separation. Only the attractive region of the potential energy surface is shown (<0 cm^{-1}) with the interval between contours set to 10 cm^{-1}.

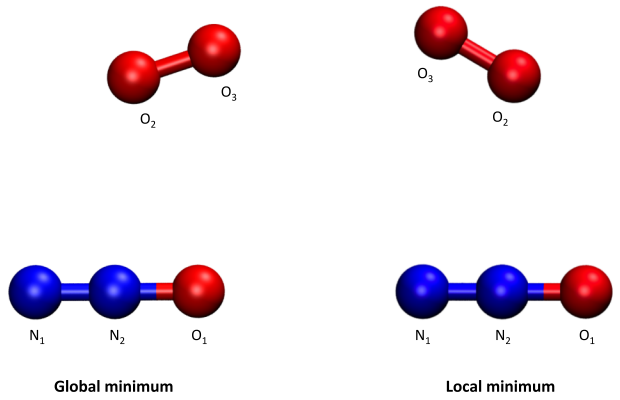

FIG. 3. The global minimum (left) and local minimum (right) structures of O_2–N_2O.

point is very flat. This means that tight convergence criteria and careful choice of numerical step-size were necessary to ensure accurate second order energy derivatives for the calculation of vibrational frequencies (Tables IV and V).

Our present *ab initio* potential energy surface has some similarities to that of Qian *et al.*, which was based on an approximate model of interaction using a combination of empirical electrostatic and Lennard-Jones potentials.[13] The corresponding multipoles for N_2O and O_2 necessary for the electrostatic interaction were obtained with the MP2/6-311G** method. Qian *et al.* identified two minima with either $\theta_1 = 123°$ and $\theta_2 = 102°$ or $\theta_1 = 62°$ and $\theta_2 = 67°$, with a first order saddle point at $\theta_1 = 90°$ and $\theta_2 = 90°$. However in contrast with our results, the former structure is calculated to be a local minimum (-159 cm^{-1}) whereas the latter is calculated to be the global minimum (-191 cm^{-1}). The potential energy surface of Qian *et al.* is also very flat, with the first order saddle point (-130 cm^{-1}) calculated to be just 61 cm^{-1} above their global minimum structure. The reversed order of the minima is attributed to the much higher level of theory used in the present investigation, afforded by the substantial improvement in computational hardware since the earlier study.

Optimized geometry

In Figure 3, we show the global and local minimum structures of O_2–N_2O. In Table I, we present the corresponding CCSD(T)-F12b optimized geometric parameters for both minima obtained with the cc-pVTZ-F12 and aug-cc-pVTZ basis sets, inclusive and exclusive of counterpoise correction.

For both minima, we find there to be almost negligible change in the intramolecular geometric parameters upon complexation. This justifies our approximation of using fixed intramolecular geometric parameters to calculate the intermolecular potential energy surface in Figure 2. The corresponding optimized values of the monomer are calculated to be R(NN) = 1.1281 Å, R(NO) = 1.1868 Å, R(OO) = 1.2068 Å, θ(NNO) = 180° with the cc-pVTZ-F12 basis set and R(NN) = 1.1281 Å, R(NO) = 1.1866 Å, R(OO) = 1.2066 Å, θ(NNO) = 180° with the aug-cc-pVTZ basis set.

In general, there is very good agreement between the optimized geometric parameters obtained with the cc-pVTZ-F12 and aug-cc-pVTZ basis sets. With exception of the intermolecular distance [$R(N_2 \cdots O_2)$], there is also relatively small variation between the standard and CP corrected optimized geometric parameters. The CP corrected intermolecular distances are consistently longer than the non-CP corrected values. This variation is larger for the aug-cc-pVTZ basis set than for the cc-pVTZ-F12 basis set, indicating that the former is more affected by basis set superposition error than the latter.

In Table II, we present the calculated interaction energies for the global and local minimum structures of O_2–N_2O obtained using the CP-corrected CCSD(T)-F12b/cc-pVTZ-F12 geometries from Table I. As expected, we find that the CP-corrected interaction energies are smaller than those calculated without counterpoise correction. This is particularly pronounced for the aug-cc-pVDZ results, which appear to suffer significantly from basis set superposition error. While the geometric parameters in Table I obtained with the cc-pVTZ-F12 and aug-cc-pVTZ basis sets are in excellent agreement with each other, there are larger differences between the corresponding interaction energies obtained with the cc-pVXZ-F12 and aug-cc-pVXZ basis sets. For a given cardinal number, we find that the interaction energies obtained with the aug-cc-pVXZ basis sets are consistently larger than those obtained with the corresponding cc-pVXZ-F12 basis sets. This variation between the basis set families is more pronounced for the interaction energies obtained without counterpoise correction. Somewhat surprisingly, the CBS extrapolated interaction energies obtained with the aug-cc-pVTZ/aug-cc-pVQZ

TABLE I. CCSD(T)-F12b optimised geometric parameters (in Å and deg) and interaction energies (in kJ mol^{-1}) for the global minimum and local minimum of O_2–N_2O.

	Global minimum				Local minimum			
	cc-pVTZ-F12		aug-cc-pVTZ		cc-pVTZ-F12		aug-cc-pVTZ	
	STD	CP	STD	CP	STD	CP	STD	CP
$R(N_1N_2)$	1.1280	1.1279	1.1279	1.1279	1.1282	1.1282	1.1282	1.1282
$R(N_2O_1)$	1.1869	1.1869	1.1867	1.1867	1.1864	1.1864	1.1861	1.1862
$R(O_2O_3)$	1.2068	1.2068	1.2067	1.2067	1.2070	1.2070	1.2069	1.2069
θ ($N_1N_2O_1$)	179.84	179.85	179.84	179.85	179.85	179.86	179.85	179.86
$R(N_2 \cdots O_2)$	3.0658	3.0806	3.0505	3.0738	3.0652	3.0802	3.0516	3.0743
θ ($N_1N_2 \cdots O_2$)	95.28	95.22	95.09	95.24	92.86	92.99	92.61	92.89
θ ($N_1N_2 \cdots O_3$)	112.67	112.46	112.66	112.55	76.36	76.83	75.66	76.48

TABLE II. CCSD(T)-F12b interaction energies (in kJ mol^{-1}) for the global minimum and local minimum of O_2–N_2O.

	Global minimum				Local minimum			
	cc-pVXZ-F12		aug-cc-pVXZ		cc-pVXZ-F12		aug-cc-pVXZ	
	STD	CP	STD	CP	STD	CP	STD	CP
Double-ζ	3.38	2.93	4.53	3.20	2.60	2.60	4.06	2.79
Triple-ζ	3.32	3.01	3.69	3.16	2.73	2.73	3.38	2.86
Quadruple-ζ	3.23	3.02	3.35	3.15	2.75	2.75	3.07	2.88
CBS		3.05		3.16		2.79		2.89
D_0[a]		1.99		2.08		1.85		1.91

[a]Calculated using the corresponding CBS limits and a zero point vibrational energy correction obtained with the CCSD(T)-F12b/cc-pVTZ-F12 or CCSD(T)-F12b/aug-cc-pVTZ harmonic frequencies from Table IV with a numerical step-size of 0.004 a.u.

basis set pair are still ~0.1 kJ mol^{-1} larger than those obtained with the cc-pVTZ-F12/cc-pVQZ-F12 basis set pair. Nonetheless for all basis sets considered, we find that the interaction energy of our global minimum structure is consistently larger than that of the corresponding local minimum structure. At the CBS limit, the global minimum structure has an interaction energy that is 0.26-0.27 kJ mol^{-1} larger than that of the local minimum structure. Inclusion of zero point vibrational energy (ZPVE) lessens the energetic difference between the local and global minima, with the difference in D_0 calculated to be 0.14-0.17 kJ mol^{-1}.

In Table III, we present the experimental vibrationally averaged Jacobi coordinates of Qian *et al.* obtained from rotationally resolved infrared spectra.[13] For comparison, we also present our optimized equilibrium structures expressed in terms of these same coordinates. In the experimental investigation, two sets of geometric parameters were found to fit the spectroscopic data equally well. The authors had a slight preference for the structure where $\theta_1 = 58°$ and $\theta_2 = 77°$, as this was in closest agreement with the global minimum structure of their calculated empirical intermolecular potential energy surface. However, this decision should be reconsidered in light of the much higher level theoretical results presented in Figure 2 and Table II, which show a reversal of the global and local minima. Furthermore, we find that the "alternate" experimental structure is in excellent agreement with our optimized global minimum structure. Despite the very flat intermolecular potential energy surface, the experimental and optimized values of θ_1 and θ_2 differ by less 2°. Agreement between the "preferred" experimental structure and the optimized local minimum structure is less good, with θ_1 and θ_2 differing by approximately 6°.

TABLE III. Comparison of the experimental and calculated Jacobi coordinates (in Å and deg).[a]

	R_{cm}	θ_1	θ_2
Experiment-preferred structure[b]	3.423	58	77
Experiment-alternate structure[b]	3.423	123	102
Global minimum			
CCSD(T)-F12b/cc-pVTZ-F12	3.332	122	104
CP CCSD(T)-F12b/cc-pVTZ-F12	3.349	121	104
CCSD(T)-F12b/aug-cc-pVTZ	3.312	121	104
CP CCSD(T)-F12b/aug-cc-pVTZ	3.342	122	104
Local minimum			
CCSD(T)-F12b/cc-pVTZ-F12	3.394	52	83
CP CCSD(T)-F12b/cc-pVTZ-F12	3.419	51	83
CCSD(T)-F12b/aug-cc-pVTZ	3.366	54	82
CP CCSD(T)-F12b/aug-cc-pVTZ	3.405	52	83

[a]Geometric parameters are defined in Figure 1.
[b]Reference 13.

While the optimized value of R_{cm} for our local minimum structure initially appears in better agreement with experiment than the global minimum structure, it must be remembered that the theoretical results are equilibrium distances (R_e) whereas the experimental value is an effective distance obtained for the ground vibrational state (R_0). Given that weakly bound complexes generally exhibit highly anharmonic intermolecular potential energy surfaces, the value of R_0 is expected to be appreciably longer than that of R_e. The N_2–CO_2 and CO–CO_2 complexes are structurally comparable to O_2–N_2O and have similar interaction energies (3.89 and 4.77 kJ mol^{-1}, respectively).[19] Our previous investigation of these complexes showed that the intermolecular distance in the vibrational ground state is approximately 0.08 Å longer than the equilibrium intermolecular distance. If we assume that this difference is transferable and add 0.08 Å to our equilibrium intermolecular distances for O_2–N_2O, we obtain estimated values for R_{cm} in the vibrational ground state of 3.39-3.43 Å for the global minimum and 3.45-3.50 Å for the local minimum. It follows that the experimentally determined intermolecular distance of 3.423 Å is then in better agreement with our global minimum structure.

Vibrational frequencies

To facilitate comparison of the geometric parameters between theory and experiment, we attempted to calculate the geometry of both the local and global minima in the vibrational ground state using the second order vibrational perturbation theory (VPT2) with the CCSD(T)/aug-cc-pVTZ method in CFOUR.[20] However despite using the tightest convergence criteria that were practicable, we were unable to calculate the necessary cubic and quartic energy derivatives with sufficient accuracy to obtain a reasonable structure. This was a somewhat surprising result, as we have previously used the same

TABLE IV. CCSD(T)-F12b/cc-pVTZ-F12 harmonic frequencies (in cm^{-1}) calculated using varying step-size for the numerical Hessian.[a]

		Step-size for numerical Hessian							
		0.001	0.002	0.003	0.004	0.005	0.006	0.008	0.010 (default)
Global minimum									
ν_1	NNO asym stretch	2287.6	2287.5	2287.5	2287.5	2287.5	2287.5	2287.6	2287.6
ν_2	OO stretch	1612.7	1612.7	1612.8	1613.0	1613.2	1613.5	1614.5	1616.1
ν_3	NNO sym stretch	1302.6	1302.5	1302.5	1302.5	1302.5	1302.5	1302.5	1302.6
ν_4	NNO in-plane bend	599.3	599.1	599.1	599.0	599.0	599.0	599.0	599.0
ν_5	NNO out-of-plane bend	599.3	599.1	599.0	599.0	599.0	598.9	598.9	598.8
ν_6	intermolecular stretch	72.7	70.7	70.2	70.0	70.0	70.3	72.7	78.7
ν_7	in-plane rock (θ_2)	51.1	47.9	46.9	45.9	44.8	43.3	38.3	26.9
ν_8	in-plane rock (θ_1)	39.1	34.5	31.9	27.3	19.6	−11.7	−43.7	−73.6
ν_9	intermolecular torsion	28.3	23.2	22.1	21.7	21.6	21.5	21.5	21.5
Local minimum									
ν_1	NNO asym stretch	2287.4	2287.4	2287.4	2287.4	2287.4	2287.4	2287.4	2287.5
ν_2	OO stretch	1606.9	1606.9	1607.0	1607.1	1607.2	1607.3	1607.8	1608.6
ν_3	NNO sym stretch	1304.0	1303.9	1303.9	1303.9	1303.9	1303.9	1303.9	1303.9
ν_4	NNO in-plane bend	600.0	599.7	599.7	599.7	599.7	599.7	599.6	599.63
ν_5	NNO out-of-plane bend	599.8	599.6	599.6	599.6	599.6	599.6	599.6	599.57
ν_6	intermolecular stretch	69.2	67.0	66.3	65.1	63.9	62.4	58.1	55.1
ν_7	in-plane rock (θ_2)	49.7	47.3	47.1	47.3	47.7	48.4	50.5	49.6
ν_8	in-plane rock (θ_1)	27.9	22.1	18.9	14.6	5.4	−14.9	−31.8	−50.3
ν_9	intermolecular torsion	29.4	22.0	20.8	20.5	20.3	20.2	20.2	20.3

[a]Obtained using the standard optimised geometric parameters from Table I.

approach to successfully determine the geometry of similar weakly bound complexes in the vibrational ground state.[19,21]

In Tables IV and V, we present harmonic frequencies for the local and global minima of O_2–N_2O calculated using varying step-sizes for the numerical Hessian. These were obtained with the CCSD(T)-F12b method and the cc-pVTZ-F12 (Table IV) and aug-cc-pVTZ (Table V) basis sets using the corresponding optimised geometric parameters from Table I. We find that the intramolecular vibrational modes ($\nu_1 - \nu_5$) exhibit variation as the step-size of the numerical

TABLE V. CCSD(T)-F12b/aug-cc-pVTZ harmonic frequencies (in cm^{-1}) calculated using varying step-size for the numerical Hessian.[a]

		Step-size for numerical Hessian							
		0.001	0.002	0.003	0.004	0.005	0.006	0.008	0.010 (default)
Global minimum									
ν_1	NNO asym stretch	2289.6	2289.5	2289.5	2289.5	2289.5	2289.6	2289.6	2289.6
ν_2	OO stretch	1617.0	1617.0	1617.2	1617.4	1617.8	1618.3	1619.8	1622.4
ν_3	NNO sym stretch	1303.9	1303.8	1303.8	1303.8	1303.8	1303.8	1303.8	1303.9
ν_4	NNO in-plane bend	601.7	601.4	601.4	601.4	601.4	601.4	601.4	601.4
ν_5	NNO out-of-plane bend	601.6	601.3	601.3	601.3	601.2	601.2	601.2	601.1
ν_6	intermolecular stretch	75.3	72.6	72.1	72.0	72.3	73.2	77.7	88.1
ν_7	in-plane rock (θ_2)	53.0	49.4	48.2	46.9	45.3	43.1	35.1	−6.1
ν_8	in-plane rock (θ_1)	40.7	25.5	24.5	23.3	−5.6	−29.4	−61.3	−99.4
ν_9	intermolecular torsion	30.7	34.2	30.4	24.1	23.9	23.9	23.8	23.8
Local minimum									
ν_1	NNO asym stretch	2289.5	2289.3	2289.3	2289.3	2289.3	2289.3	2289.3	2289.36
ν_2	OO stretch	1609.9	1609.6	1609.7	1609.8	1609.9	1610.2	1610.9	1612.06
ν_3	NNO sym stretch	1305.7	1305.3	1305.2	1305.2	1305.2	1305.2	1305.2	1305.25
ν_4	NNO in-plane bend	602.9	602.2	602.1	602.0	602.0	601.9	601.9	601.92
ν_5	NNO out-of-plane bend	602.6	602.2	602.0	602.0	601.9	601.9	601.9	601.89
ν_6	intermolecular stretch	77.6	70.9	68.8	67.3	65.7	63.6	58.0	46.13
ν_7	in-plane rock (θ_2)	57.9	50.6	49.2	49.1	49.6	50.4	52.8	59.09
ν_8	in-plane rock (θ_1)	42.8	27.4	21.3	15.0	−7.5	−20.5	−40.1	−63.1
ν_9	intermolecular torsion	37.3	27.3	24.4	23.2	22.6	22.3	22.1	22.02

[a]Obtained using the standard optimised geometric parameters from Table I.

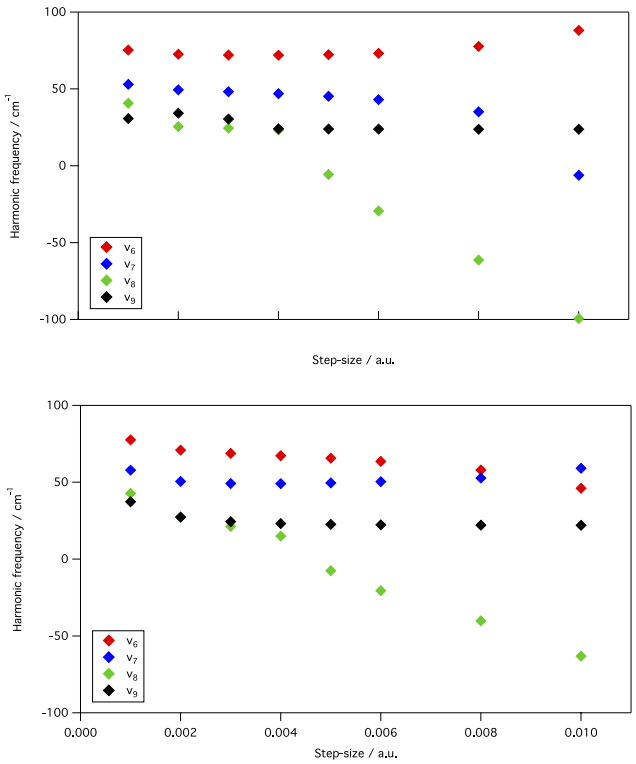

FIG. 4. The CCSD(T)-F12b/aug-cc-pVTZ intermolecular vibrational frequencies of O_2–N_2O obtained with varying step-size for the numerical Hessian. Global minimum (top) and local minimum (bottom).

Hessian decreases from the default value of 0.010 a.u.–0.001 a.u. The vibrational modes of the N_2O sub-unit (ν_1 and ν_3–ν_5) are only slightly perturbed from their monomeric values,[22] with the important asymmetric bending mode being 599.0 cm^{-1} and 601.5 cm^{-1} with the CCSD(T)-F12b/cc-pVTZ-F12 and CCSD(T)-F12b/aug-cc-pVTZ methods.

We find that the intermolecular vibrational modes (ν_6 – ν_9) exhibit much larger variation than the intramolecular modes. Of greatest concern is that with the default step-size, both the local and global minima and calculated with either the cc-pVTZ-F12 or aug-cc-pVTZ basis sets exhibit one or two imaginary frequencies. The intermolecular vibrational modes of the local and global minima are qualitatively similar. The ν_6 mode corresponds to the intermolecular stretch, the ν_7 mode corresponds to an in-plane rock following the θ_2 coordinate, the ν_8 mode corresponds to an in-plane rock following the θ_1 coordinate, and the ν_9 mode corresponds to an out-of-plane intermolecular torsion. In Figure 4, we plot the intermolecular vibrational frequencies of the local and global minimum obtained with the CCSD(T)-F12b/aug-cc-pVTZ method. The corresponding results for the CCSD(T)-F12b/cc-pVTZ-F12 method are shown in the supplementary material.[22] We find that the ν_6 and ν_9 modes are generally well behaved as the step-size of the numerical Hessian changes. However, the ν_7 and ν_8 modes exhibit much greater variation. While it is difficult to confidently state our best estimate of the harmonic vibrational frequencies for O_2–N_2O, the results seem to be largely converged with a step-size of 0.002-0.004 a.u. Use of a smaller step-size appears to result in problems with numerical instability, as the displacement creates an energetic change that is of comparable magnitude to the single-point convergence criteria. However, use of a larger step-size is clearly resulting in some unphysical results for the in-plane ν_7 and ν_8 vibrational modes.

To investigate this issue further, we have also optimized the global and local minimum structures of O_2–N_2O

TABLE VI. CCSD(T)/aug-cc-pVTZ harmonic frequencies (in cm^{-1}) calculated using varying step-size for the numerical Hessian.[a]

		Step-size for numerical Hessian							
		0.001	0.002	0.003	0.004	0.005	0.006	0.008	0.010 (default)
Global minimum									
ν_1	NNO asym stretch	2267.3	2267.2	2267.2	2267.2	2267.2	2267.2	2267.2	2267.3
ν_2	OO stretch	1580.0	1579.9	1579.9	1580.0	1580.0	1580.1	1580.3	1580.6
ν_3	NNO sym stretch	1286.7	1286.6	1286.6	1286.6	1286.6	1286.6	1286.6	1286.6
ν_4	NNO in-plane bend	593.4	593.2	593.2	593.1	593.1	593.1	593.1	593.1
ν_5	NNO out-of-plane bend	592.9	592.7	592.6	592.6	592.6	592.6	592.5	592.5
ν_6	intermolecular stretch	77.0	75.0	74.7	74.5	74.4	74.3	74.2	74.3
ν_7	in-plane rock (θ_2)	54.3	51.7	51.1	50.7	50.4	50.0	49.2	47.9
ν_8	in-plane rock (θ_1)	37.9	34.2	32.8	31.9	30.6	28.9	23.7	11.5
ν_9	intermolecular torsion	30.7	26.2	25.3	25.0	24.8	24.8	24.8	24.8
Local minimum									
ν_1	NNO asym stretch	2267.1	2267.0	2267.0	2267.0	2267.1	2267.1	2267.1	2267.1
ν_2	OO stretch	1576.4	1576.3	1576.3	1576.4	1576.4	1576.5	1576.4	1576.7
ν_3	NNO sym stretch	1287.8	1287.7	1287.7	1287.7	1287.7	1287.7	1287.8	1287.8
ν_4	NNO in-plane bend	593.9	593.6	593.6	593.6	593.6	593.6	593.5	593.6
ν_5	NNO out-of-plane bend	593.5	593.3	593.2	593.2	593.2	593.2	593.2	593.2
ν_6	intermolecular stretch	76.0	74.1	73.8	73.5	73.2	73.1	70.6	70.7
ν_7	in-plane rock (θ_2)	51.3	49.0	48.4	48.3	48.3	47.9	50.7	49.4
ν_8	in-plane rock (θ_1)	30.2	26.1	24.7	24.4	24.3	24.2	12.0	24.2
ν_9	intermolecular torsion	28.9	23.3	22.4	21.2	20.0	20.0	−1.7	−4.9

[a]Obtained using the CCSD(T)/aug-cc-pVTZ standard optimised geometric parameters I.

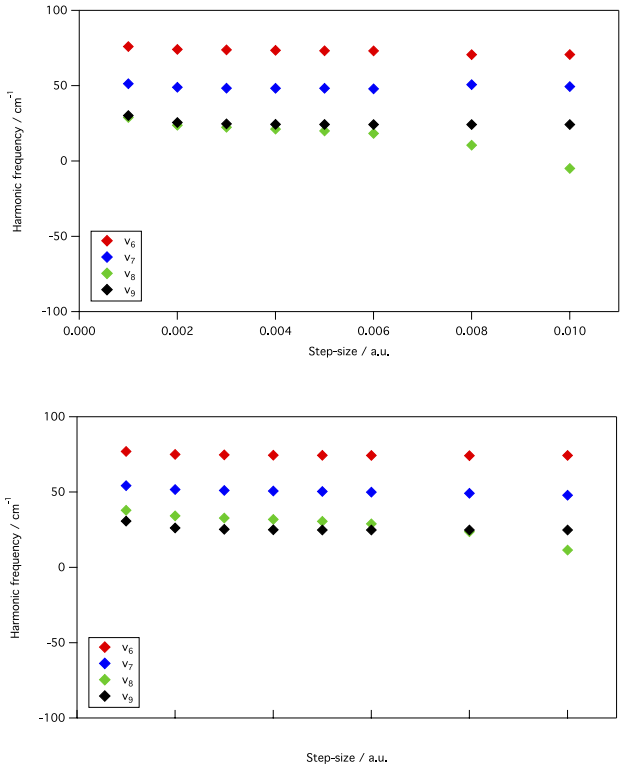

FIG. 5. The CCSD(T)/aug-cc-pVTZ intermolecular vibrational frequencies of O_2–N_2O obtained with varying step-size for the numerical Hessian. Global minimum (top) and local minimum (bottom).

and calculated the corresponding vibrational frequencies with conventional coupled cluster theory. In Table VI, we present these CCSD(T)/aug-cc-pVTZ harmonic vibrational frequencies obtained with varying step-size for the numerical Hessian. Interestingly, we find that the vibrational frequencies obtained with the CCSD(T)/aug-cc-pVTZ method exhibit much less variation as the step-size of the numerical Hessian changes as compared to the CCSD(T)-F12b/aug-cc-pVTZ or CCSD(T)-F12b/cc-pVTZ-F12 results. This behaviour is particularly pronounced for the intermolecular vibrational modes and is shown graphically in Figure 5.

The conventional CCSD(T)/aug-cc-pVTZ vibrational frequencies appear to be largely converged with a wide range of step-size from 0.002-0.008 a.u. For step-sizes of 0.002-0.004, where both the CCSD(T) and CCSD(T)-F12b results appear to be converged, there is good agreement between the vibrational frequencies calculated with the CCSD(T)-F12b/cc-pVTZ-F12, CCSD(T)-F12b/aug-cc-pVTZ, and CCSD(T)/aug-cc-pVTZ methods. While all three methods exhibit qualitatively similar intermolecular potential energy surfaces (Figures S1-S3 of the supplementary material),[22] the CCSD(T)/aug-cc-pVTZ method has deeper energy wells due to basis set superposition error, which is substantially larger with conventional CCSD(T) than explicitly correlated CCSD(T)-F12.[19,23,24] Note that as the vibrational frequencies are evaluated without counterpoise correction, it is the non-counterpoise corrected interaction energies that should be compared. We find that the non-counterpoise corrected CCSD(T)/aug-cc-pVTZ interaction energy of the global minimum is 4.15 kJ mol^{-1} whereas the local minimum is 3.89 kJ mol^{-1}. These values are appreciably larger than the corresponding non-counterpoise corrected interaction energies in Table II obtained with the CCSD(T)-F12/cc-pVTZ-F12 and CCSD(T)-F12b/aug-cc-pVTZ methods. We therefore suggest that the variability in the low frequency intermolecular vibrational modes in Tables IV and V is primarily due to the extremely flat intermolecular potential energy surface.

CONCLUSIONS

We have constructed a counterpoise corrected intermolecular potential energy surface for the O_2–N_2O complex using the CCSD(T)-F12b/aug-cc-pVTZ method. Similar to earlier work by Qian *et al.*, we find there to be two minima of comparable energy (3.15 and 2.86 kJ mol^{-1}) that are separated by a low energy first order saddle point. However, our present results show that the earlier assignment of the local and global minima is likely incorrect and should be swapped. This has implications for the currently preferred experimental structure of O_2–N_2O determined from rotationally resolved infrared spectra. As two sets of geometric parameters equally fit the spectroscopic data, the structure of O_2–N_2O in closest agreement with the earlier calculated global minimum was favoured. While this was a sensible decision, the present much more accurate theoretical results should now be used to arbitrate between the two possible experimental structures. We find that our present optimized global minimum structure is in excellent agreement with the less preferred experimental structure and conclude that experimental geometric parameters of O_2–N_2O are in fact $\theta_1 = 123°$, $\theta_2 = 102°$, and $R_{cm} = 3.423$ Å . Finally, we have shown that the very flat potential energy surface of O_2–N_2O surrounding the local and global minima is problematic when evaluating vibrational frequencies with a numerical Hessian. This highlights the need for at least consideration of how the calculated vibrational frequencies might vary as the Hessian step-size is changed.

ACKNOWLEDGMENTS

We thank the Marsden Fund administered by the Royal Society of New Zealand for funding and the University of Waikato High Performance Computing Facility for computer time. We thank K. M. de Lange for undertaking preliminary calculations.

[1]A. R. Ravishankara, J. S. Daniel, and R. W. Portmann, Science **326**, 123 (2009), ISSN 1095-9203.
[2]IPCC, in *Climate Change 2013*, edited by T. Stocker, D. Qin, G.-K. Plattner, M. Tignor, S. Allen, J. Boschung, A. Nauels, Y. Xia, V. Bex, and P. Midgley (IPCC, Geneva, Switzerland, 2013), p. 1535.
[3]J. Huang, A. Golombek, R. Prinn, R. Weiss, P. Fraser, P. Simmonds, E. J. Dlugokencky, B. Hall, J. Elkins, P. Steele *et al.*, J. Geophys. Res. **113**, D17313, doi:10.1029/2007JD009381 (2008), ISSN 0148-0227.
[4]A. Syakila and C. Kroeze, Greenhouse Gas Meas. Manage. **1**, 17 (2011), ISSN 2043-0779.
[5]R. Spahni, J. Chappellaz, T. F. Stocker, L. Loulergue, G. Hausammann, K. Kawamura, J. Flückiger, J. Schwander, D. Raynaud, V. Masson-Delmotte *et al.*, Science **310**, 1317 (2005), ISSN 1095-9203.
[6]C. M. Volk, J. W. Elkins, D. W. Fahey, G. S. Dutton, J. M. Gilligan, M. Loewenstein, J. R. Podolske, K. R. Chan, and M. R. Gunson, J. Geophys. Res. **102**, 25543, doi:10.1029/97JD02215 (1997), ISSN 0148-0227.
[7]N. Rontu Carlon, D. K. Papanastasiou, E. L. Fleming, C. H. Jackman, P. A. Newman, and J. B. Burkholder, Atmos. Chem. Phys. **10**, 6137 (2010), ISSN 1680-7324.

[8]R. Schinke, J. Chem. Phys. **134**, 064313 (2011), ISSN 1089-7690.
[9]J. A. Schmidt, M. S. Johnson, and R. Schinke, Atmos. Chem. Phys. **11**, 8965 (2011), ISSN 1680-7324.
[10]W. Klemperer and V. Vaida, Proc. Natl. Acad. Sci. U. S. A. **103**, 10584 (2006), ISSN 0027-8424.
[11]L. Brown and V. Vaida, J. Phys. Chem. **100**, 7849 (1996), ISSN 0022-3654.
[12]M. Bahou, L. Schriver-Mazzuoli, C. Camy-Peyret, A. Schriver, T. Chiavassa, and J. Aycard, Chem. Phys. Lett. **265**, 145 (1997), ISSN 00092614.
[13]H.-B. Qian, D. Seccombe, and B. J. Howard, J. Chem. Phys. **107**, 7658 (1997), ISSN 0021-9606.
[14]S. Li, R. Zheng, and C.-X. Duan, Chin. Phys. B **23**, 123301 (2014), ISSN 1674-1056.
[15]H. J. Werner, P. J. Knowles, G. Knizia, F. R. Manby, and M. Schütz, Wiley Interdiscip. Rev.: Comput. Mol. Sci. **2**, 242 (2012), ISSN 17590876.
[16]S. Simon, M. Duran, and J. J. Dannenberg, J. Chem. Phys. **105**, 11024 (1996), ISSN 00219606.
[17]J. G. Hill, K. A. Peterson, G. Knizia, and H.-J. Werner, J. Chem. Phys. **131**, 194105 (2009), ISSN 1089-7690.
[18]D. W. Schwenke, J. Chem. Phys. **122** (2005), ISSN 00219606.
[19]K. M. De Lange and J. R. Lane, J. Chem. Phys. **134**, 034301 (2011), ISSN 00219606.
[20]J. Stanton, J. Gauss, M. Harding, and P. Szalay, CFOUR, a quantum chemical program, http://www.cfour.de.
[21]J. D. McMahon and J. R. Lane, J. Chem. Phys. **135**, 154309 (2011), ISSN 00219606.
[22]See supplementary material at http://dx.doi.org/10.1063/1.4931629 for intermolecular potential energy surfaces obtained with the CCSD(T) and CCSD(T)-F12 methods; harmonic vibrational frequencies of N_2O monomer.
[23]J. R. Lane and H. G. Kjaergaard, J. Chem. Phys. **131**, 1 (2009), ISSN 00219606.
[24]J. R. Lane, J. Chem. Theory Comput. **9**, 316 (2013), ISSN 15499618.